SQUID linearization by current-sampling feedback

Mikko Kiviranta
VTT, Tietotie 3, 02150 Espoo, Finland

E-mail: Mikko.Kiviranta@vtt.fi

Abstract. Local negative feedback derived within the cryogenic stage from the output current of a voltage-biased SQUID series array is used to linearize the flux response and to simultaneously approach the noise matching resistance of the room-temperature readout amplifier. The flux noise level of the SQUID array was 0.5 $\mu\Phi_0/\mathrm{Hz}^{1/2}$ in open loop and 0.8 $\mu\Phi_0/\mathrm{Hz}^{1/2}$ in the feedback arrangement having a 2.2 Φ_0 peak-to-peak flux locking range. The noise level degraded to 2 $\mu\Phi_0/\mathrm{Hz}^{1/2}$ in an arrangement with a 7 Φ_0 locking range. Very good linearity was observed in the feedback system regardless of the modest loop gain, owing to the open-loop SQUID characteristics which are more linear in voltage biased than current biased case. Upward and downward slew rates of 3.4 and 1.2 $\Phi_0/\mu\mathrm{s}$ were recorded which, however, do not represent ultimate limits of the approach. Local feedback schemes are reviewed and their effect on the linearity of a SQUID system is discussed.

1. Introduction

[*]When utilizing dc SQUIDs[1] in practical circuits two commonly encountered problems are (i) providing noise match to the room temperature amplifier following the SQUID and (ii) linearizing the naturally non-linear flux response of the SQUID. The positive feedback method APF [1] and noise cancellation method NC [2, 3] have been utilized in the past to boost the SQUID output impedance to more closely match the room temperature amplifier. Negative feedback is then applied, typically in the form of the FLL [4] in order to linearize the response. The feedback signal is typically derived from the output of the room temperature amplifier, where the signal has been amplified sufficiently so that the reduction in the signal strength due to the negative feedback can be tolerated without encountering noise matching problems with further amplifier stages. A consequence is that the delay in the cables connecting the SQUID and the room temperature amplifier tends to limit the obtainable bandwidth.

The simple linear amplifier theory [5] describes two ways to derive the negative feedback signal from the amplifier output: voltage sampling which tends to decrease the output impedance, and current sampling which tends to increase it. For positive feedback the effects are opposite. The techniques are of course applicable to SQUIDs [6], in which context the current-sampling negative feedback has the attractive feature that it simultaneously linearizes the SQUID response and increases the SQUID dynamic resistance, which typically is too low for obtaining a noise match with the room temperature amplifier. If the feedback is derived from the SQUID output rather than from the output of the room temperature amplifier, the delay in the feedback loop is greatly reduced.

This work describes our first experimental results on the current-sampling feedback scheme, proposed in [7] for the application of Frequency Domain Multiplexing (FDM) of Transition Edge Calorimeter sensors.

2. Theoretical considerations

2.1 Linearization

Dynamic range D of a SQUID system can be defined as the ratio of the maximum peak-to-peak flux excursion, whose response at the SQUID output does not exceed a prescribed nonlinearity level, to the RMS flux noise over unit bandwidth.

---

[*] This paper has been published as *Supercond. Sci. Tech.* **21** (2008) 045009, http://stacks.iop.org/0953-2048/21/045009

[1] SQUIDs and SQUID arrays can be treated on equal footing by noting that a k-SQUID series array, whose each constituent SQUID has loop inductance L_{SQ} , junction capacitance C_J and is coupled to a m-turn input coil, has the same circuit parameters as a single SQUID with loop inductance L_{SQ}/k, junction capacitance kC_J, a km-turn input coil and a 1:k transformer at its output.

When specifying rf circuitry, for example, it is customary to use the –1 dB gain suppression as the nonlinearity prescription. In the typical case of FDM readout of X-ray calorimeters [8] it is more relevant to require the SQUID gain to deviate by less than a factor $\Delta E/E$ from a strictly linear response. In our application, $\Delta E/E$ is the ratio of the maximum X-ray photon energy to the desired energy resolution. For our desired resolution, this implies the suppression or enhancement of the SQUID output of no more than 0.01 dB. An idea of the typical tolerable flux excursion for a SQUID without additional circuitry can be obtained by performing a numerical fit to the SQUID characteristics shown in Figure 5 and Figure 6. A fit to the middle of the rising slope of the current-biased SQUID at I_B = 60 μA (Figure 6) results in $U(\phi) = 322\,\mu\mathrm{V} + 5.60\,\mathrm{mV} \times (\phi + 7\phi^2 - 20\phi^3)$, indicating a 0.01 dB-accurate peak-to-peak flux range of $\sim 1.5\times10^{-4}\Phi_0$. The voltage-biased SQUID (Figure 7) is significantly more linear, the fitted response in the falling slope being $I(\phi) = 64\mu\mathrm{A} - 144\mu\mathrm{A} \times (\phi + 0.6\phi^2 - 2.2\phi^3)$, which indicates an order-of-magnitude larger flux range. ϕ is the applied flux expressed in the units of flux quanta Φ_0. Note that the rising slope in the current biased case corresponds to the same flux range as the falling slope in the voltage biased case.

There are a number of ways to improve the linear flux range, including (i) calibrate-and-correct methods, (ii) the fine-coarse feedforward [8,9] and (iii) negative feedback. Calibrate-and-correct methods employ measurement of the non-linear SQUID response with a known calibration signal and correcting the actual signal based on the calibration. If the frequency content of the calibration signal can be located above the signal band it becomes possible to perform calibration in a continuous manner, simultaneously with the actual signal measurement. An advantage of the method in the context of multiplexing systems is that de-multiplexing of the feedback is not necessary but the calibration signal can be fed to all the channels, the chosen forward multiplexing scheme taking care of distinguishing the calibration signals which belong to different channels. An example is a method [10] in which an L-SQUID generates both $sin\Phi$– and $cos\Phi$-like responses, whose coefficients can be intepreted as two samples of an underlying ad hoc model of the SQUID response. A straightforward way to obtain the $sin\Phi$– and $cos\Phi$ –like responses from a dc SQUID is to add a rectangular $\Phi_0/4$-amplitude modulation on top of the measured signals. Obtaining more than two samples of the SQUID

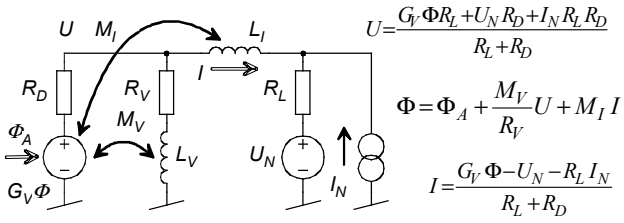

Figure 1: Network equations of the SQUID with feedback

response for calibration is the obvious generalization, and ultimately it may be possible to measure the full continuous SQUID response for calibration [11].

The more traditional linearization method is negative feedback, a local version of which is studied in this paper. By equating coefficients of a third-order Taylor expansion in the network equations of a feedback circuit, one obtains the result that the open loop SQUID response

$$s(\phi) = G(\phi + a\phi^2 + b\phi^3) \qquad (1)$$

becomes

$$s(\phi) = \frac{G}{\mathscr{L}+1}\left(\phi + \frac{a}{(\mathscr{L}+1)^2}\phi^2 + \left(\frac{b}{(\mathscr{L}+1)^3} + \frac{2a^2\mathscr{L}}{(\mathscr{L}+1)^4}\right)\phi^3\right) \qquad (2)$$

when negative feedback with loop gain $-\mathscr{L}$ is applied. In practical SQUID feedback systems the $\mathscr{L}$ is a function of frequency, however. The above equation only holds when the constant-$\mathscr{L}$ region in the frequency response of the circuit is designed to include also the harmonics generated by the ϕ^2 and ϕ^3 terms in addition to the fundamental signal frequency.

2.2 The local feedback circuit

In the electrical circuit depicted in Figure 1 the SQUID is modelled as a flux dependent voltage source with flux-to-voltage transfer coefficient G_V and dynamic resistance R_D. The total applied flux Φ is a sum of the external signal flux Φ_A and feedback fluxes due to mutual inductances M_I and M_V. R_L is the input resistance of the readout amplifier, whereas U_N and I_N are a small test voltage and a test current ultimately to be replaced by noise sources. For simplicity the R_V-L_V circuit is assumed not to draw current and L_I is assumed not to cause a voltage drop. The solutions of the network equations are

$$I = \frac{\Phi_A G_V - (U_N + I_N R_L)(1 - \mathscr{L}_V)}{R_L(1 - \mathscr{L}_V) + R_D(1 - \mathscr{L}_I)} \qquad (3)$$

and

$$\Phi = \frac{\Phi_A (R_L + R_D) + (U_N + I_N R_L)\frac{R_D}{G_V}(\mathscr{G}_V - \mathscr{G}_I)}{R_L(1-\mathscr{G}_V) + R_D(1-\mathscr{G}_I)} \quad (4)$$

expressed in terms of the voltage-mode loop gain $\mathscr{G}_V = M_V G_V / R_V$ and the current-mode loop gain $\mathscr{G}_I = M_I G_V / R_D$. Positive feedback occurs when $\{\mathscr{G}_I > 0$, not $R_L >> R_D\}$ or $\{\mathscr{G}_V > 0$, not $R_L << R_D\}$, in which case the total flux (eq. 4) becomes larger than the external flux indicating reduced SQUID dynamic range. Note that in SQUIDs G_V and therefore the polarity of the feedback changes sign at $\Phi_0/2$ intervals of the total flux. Note also that appearance of U_N and I_N in eq. (4) implies that the amplifier noise gets coupled to the SQUID and may act back on the device which the SQUID reads.

By applying a small test voltage U_N (test current I_N) and considering the evoked current (voltage) at the load R_L one obtains the effective dynamic resistance of the SQUID with the feedback circuit

$$R_{D,eff} = R_D \frac{\mathscr{G}_I - 1}{\mathscr{G}_V - 1}. \quad (5)$$

Power gain, or strictly speaking the flux-to-power transfer coefficient of the circuit to the optimal load $R_L = R_{D,eff}$ is

$$\frac{dP}{d\Phi_A^2} = \frac{G_V^2}{4R_D} \cdot \frac{1}{1 - \mathscr{G}_V - \mathscr{G}_I + \mathscr{G}_V \mathscr{G}_I}, \quad (6)$$

which determines the noise power delivered to the amplifier input R_L due to the SQUID flux noise, i.e. the required noise temperature of the readout.

Eq. (5) indicates that modification of $R_{D,eff}$ to better noise match the readout amplifier is possible. This has been performed in the past by using $0 < \mathscr{G}_V < 1$ and $\mathscr{G}_I = 0$ under the name APF [1] in the case $R_L = \infty$ and under the name NC [2, 3] in the case $R_L = 0$. Even though the eqs. (5,6) which determine the noise matching do *not* depend on R_L, the eq. (4) *does*, which leads to a profound difference in linearity between the APF and NC[2] (see Figure 2).

Drung has also pioneered the clever combination of APF together with the choice $0 < L_I < 1$ under the name BCF [12], which reduces $R_{D,eff}$ compared to the pure-APF case but increases the total power gain of the SQUID (eq. 6). In this paper we consider the case $L_I < 0$ and $R_L = 0$ as a means to simultaneously improve the noise match to the readout amplifier and linearize the SQUID response.

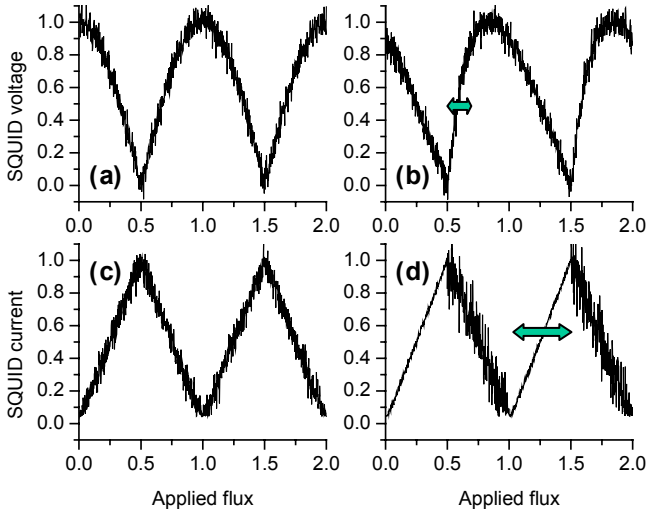

Figure 2: Simulated effect of the Drung-style APF and Seppä-style NC on the flux response of the SQUID, with exaggerated readout amplifier noise. The current biased SQUID response (a) gets modified when APF is applied (b), resulting in an unchanged noise contribution but greater gain for the flux signal. The voltage biased SQUID response (c) does not change when NC is applied (d), but the noise contribution cancels away on one slope and gets enhanced on the other slope. The useable flux range is indicated by arrows.

3. Experiments

3.1 Setup

Electronics setup is based on our standard 1 MHz-bandwidth voltage-biasing electronics [13] coupled to an additional cold circuit card as depicted in Figure 3. The bias voltage of the SQUID is generated over the R_2 = 22 Ω resistor by passing current through it. The AD797 operational amplifier is configured as a transimpedance amplifier whose zero-impedance input node is created on the cold circuit card at the point where the R_3 feedback resistor connects to the non-inverting input of the opamp. The current sampling flux feedback is activated by a cryogenic CMOS switch. The additional inductor L_1 = 8.2 μH together with R_1 = 100 Ω forms a loop filter which cuts off the flux feedback at high frequencies where the R_3-mediated transimpedance feedback cannot keep the input node at zero impedance any more. The R_1 was chosen such that its Johnson noise feeding the

[2] A viewpoint can be adopted that Noise Cancellation is *not* a (positive) feedback method, in the sense that applied external (signal) flux does not give rise to any additional flux through any feedback mechanism.

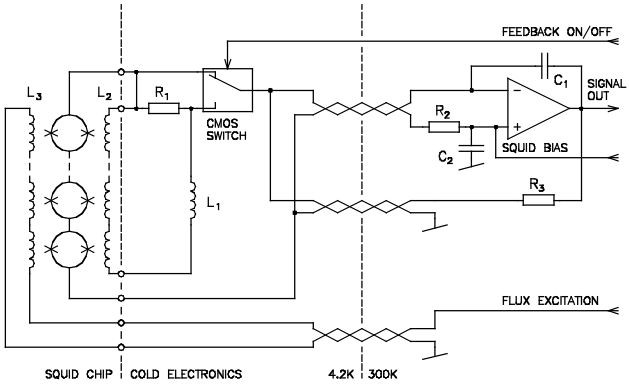

Figure 3: Simplified schematic of the experimental circuit.

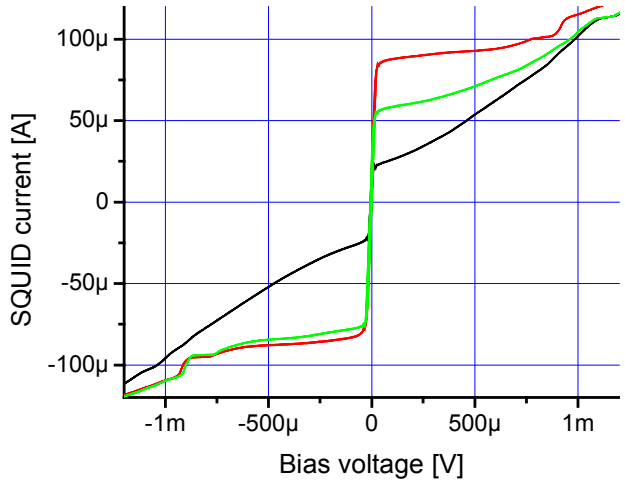

Figure 4: Voltage-to-current characteristics of the SQUID array at approximate applied flux of $N\,\Phi_0$, $(N+¼)\Phi_0$ and $(N+½)\Phi_0$.

feedback coil would contribute negligibly to the total flux noise.

The SQUID device is an annealed 16-SQUID series array described in [14], fabricated by a process overviewed in ref. [15]. The device has two tight-coupled input coils with inverse mutual inductances of M_A^{-1} = 9 µA/Φ_0 and M_B^{-1} =36 µA/Φ_0, and a loose-coupled coil with M_{FB}^{-1} = 38 µA/Φ_0. Voltage-to-current characteristics of the device, measured with the voltage-biasing setup are shown in Figure 4. The flux-to-current characteristics are shown in in Figure 5. The SQUID bias circuit has the resistance of the CMOS switch~0.2 Ω coupled in series, so that the bias condition is not strictly voltage-like. In the cryogenic setup the bond wires go over the intermediate transformer present on the SQUID chip, causing a certain amount of SQUID current to couple as magnetic flux to the SQUID input. The current-biased flux-to-voltage characteristics of the device have been measured before [14] and are shown for comparison in Figure 6.

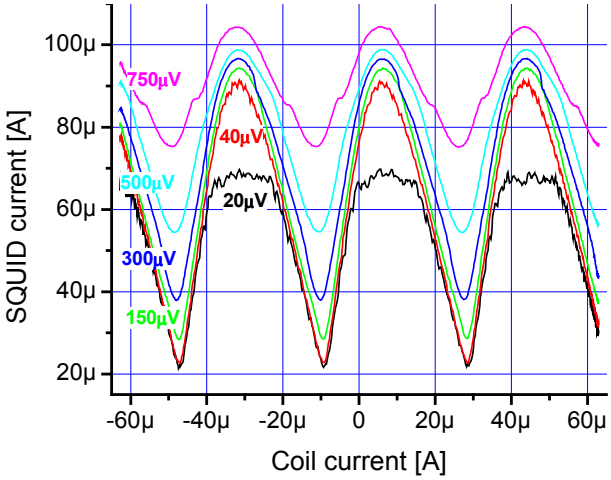

Figure 5: Flux-to-current characteristics of the SQUID array at bias voltages U_b = 20µV, 40µV, 150µV, 300µV, 500µV and 750µV. The noisy response at two lowest bias voltages is due to the vicinity of the superconducting transition.

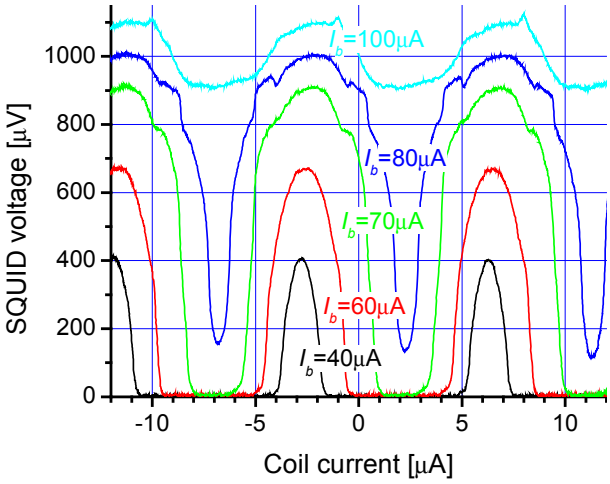

Figure 6: Flux-to-voltage characteristics of the SQUID array at various bias currents.

3.2 Results

The first set of experiments was performed using the M^{-1} = 36 µA/Φ_0 coil for the flux feedback and the second set using the M^{-1} = 9 µA/Φ_0 coil. The flux excitation was applied through the loose-coupled M^{-1} = 38 µA/Φ_0 coil in both cases. The SQUID setup reached the flux noise level of the order of 0.5 $\mu\Phi_0/\mathrm{Hz}^{1/2}$ (Figure 9) at U_b = 150 µV bias voltage typically used in the experiments when the flux feedback was not activated. This demonstrates that low-noise operation of the SQUID array in a voltage-biased mode is feasible. Our numerical simulations suggest that the inductive impedance presented by bond wires and other parasitic series inductors at Josephson frequencies causes mode-locking of the constituent SQUIDs, at least in the case where the

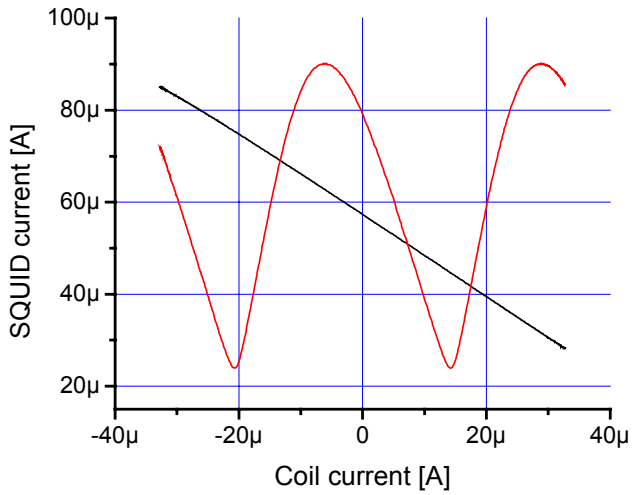

Figure 7: The current response of the voltage biased SQUID array to the applied flux, with and without the feedback activated. The feedback is applied through the M^{-1} = 36 µA/Φ_0 input coil.

dimensions of the SQUID array are shorter than the wavelength of the Josephson oscillation propagating through the array structure.

The system with M^{-1} = 36 µA/Φ_0 feedback typically unlocked when the flux amplitude exceeded 2.2 Φ_0 p-p. When the feedback was active the slope midpoint was found by keeping the flux modulation of maximal amplitude switched on and adjusting the offset flux until the unlocking symptoms occurred symmetrically on both edges of the modulation range. Slight reduction of the flux amplitude then resulted in a very linear response (Figure 7). Numerical fit to the response

$$I(\phi) = 54\,\mu\text{A} - 31\,\mu\text{A} \cdot \left(\phi + 0.016\phi^2 - 0.026\phi^3\right)$$

indicates 0.01dB suppressed flux range of 0.06 Φ_0 p-p. Quick deviation from the linear response when the flux excitation amplitude was increased is likely to be caused by the abrupt approach of the turning points in the open-loop flux characteristics. Using a 1.5 Φ_0 p-p square wave at 100 kHz as the excitation resulted in 3.4 Φ_0/µs slew rate in the rising edge and 1.2 Φ_0/µs in the falling edge. The modest slew rate values are likely to be caused by the conservative dimensioning of the R_1-L_1 loop filter due to the low bandwidth (nominally 1 MHz) of the transconductance amplifier. Increase of the flux noise to 0.8 µΦ_0/Hz$^{1/2}$ was observed with the feedback active (Figure 9).

The system with M^{-1} = 9 µA/Φ_0 feedback had the maximum locking flux range of approximately 7 Φ_0 p-p. The flux response to a 6.5 Φ_0 p-p excitation with the feedback switched

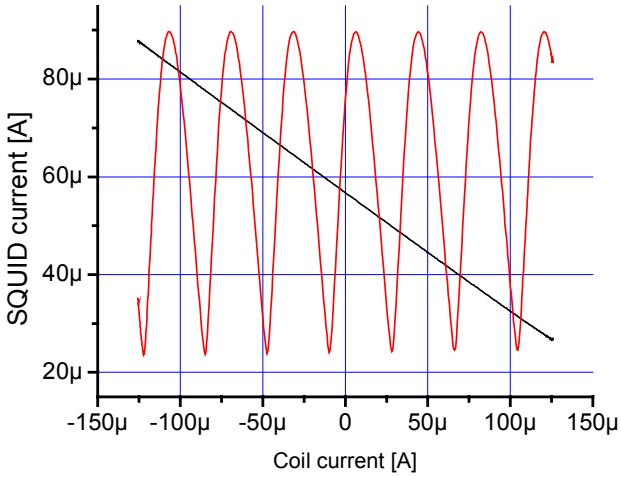

Figure 8: The current response of the SQUID array to the applied flux, with and without feedback activated. The feedback is applied through the M^{-1} = 9 µA/Φ_0 input coil.

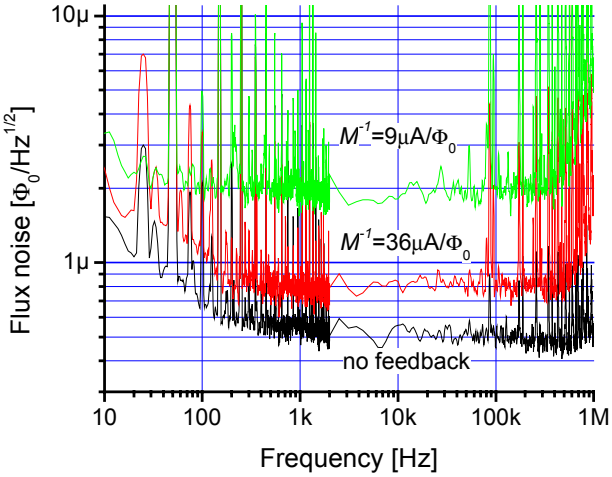

Figure 9: Input referred flux noise of the SQUID array without feedback and with feedback at two different loopgain values.

on and off is shown in Figure 8. The response with active feedback was numerically fitted as

$$I(\phi) = 57\,\mu\text{A} + 9.3\,\mu\text{A} \cdot \left(\phi + 0.004\phi^2 - 0.001\phi^3\right)$$

indicating 0.01dB suppressed flux range of 0.25 Φ_0 p-p. Again, an anomalous increase of flux noise to 2 µΦ_0/Hz$^{1/2}$ was observed when the feedback is active (Figure 9).

4. Discussion

Even with the excess noise present, the 0.01dB gain suppression limited dynamic range of the SQUID system increases from $D_{0.01\text{dB}}$ = 3 300 Hz$^{1/2}$ in the open-loop case to $D_{0.01\text{dB}}$ = 75 000 Hz$^{1/2}$ when feedback is applied through the M^{-1} = 36 µA/Φ_0 coil and further to $D_{0.01\text{dB}}$ = 125 000 Hz$^{1/2}$ when feedback is applied through the

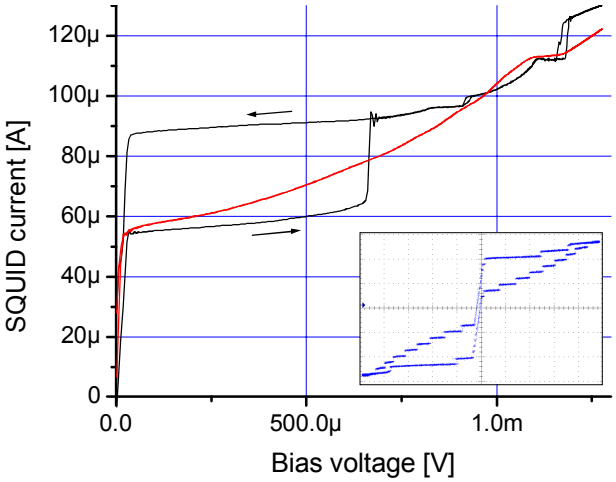

Figure 10: The voltage-to-current characteristics of the SQUID array at applied flux of approximately $(N+¼)\Phi_0$ and 150 µV bias, with and without feedback activated. The feedback is applied through the M^{-1} = 36 µA/Φ_0 coil. The inset shows the voltage-to-current characteristics when the feedback is applied through the M^{-1} = 9 µA/Φ_0 coil. The plateaus correspond to the regions of negative flux feedback and are verticlly separated by the current corresponding a one-Φ_0 flux jump. Vertical sections occur in the curve when the flux value enters the positive-feedback region.

M^{-1} = 9 µA/Φ_0 coil. The measured nonlinearity coefficients remain within a factor of two of the theoretical values estimated through eq. (2).

A conceivable reason for the observed excess flux noise is that the flux feedback increases the $R_{D,eff}$ (eq. 5) of the SQUID above the specified noise matching resistance ~450 Ω of the AD797 opamp so that the current noise rather than voltage noise of the amplifier begins to dominate. The enhancement of R_D = 45 Ω to $R_{D,eff}$ = 115 Ω at the U_b = 150 µV setpoint while feeding back through the M^{-1} = 36 µA/Φ_0 coil can be observed directly in the SQUID characteristics depicted in Figure 10. The loop gains estimated locally at the SQUID setpoint as $\mathcal{G}_I$ = -4 and $\mathcal{G}_I$ = -16 indicate (eq. 5) that the matching resistance of the AD797 is indeed approached in the former and exceeded in the latter case, but the observed amount of excess noise can be explained only if more current noise is fed to the SQUID than indicated by the AD797 noise specification.

The deep reason behind the excess noise is the fact that any linearizing (i.e. negative) local feedback scheme reduces the signal power (eq. 6) at the SQUID output, ultimately to the extent that the signal power gets overwhelmed by the readout amplifier noise. A better alternative is to use as the second stage a device whose dynamic range window, defined by its noise floor and its nonlinearity-limited maximum signal level, is at least as wide as that of the SQUID but occurs at larger signal power levels. For example a cryogenic semiconductor amplifier can be used as the second stage [16] for boosting the open-loop power gain so that a fraction of it can be lost for linearization purposes without sacrifying the capability to drive the subsequent stage.

Even though improvement of the setup described here is possible, attempts to increase the bandwidth and slew rate will ultimately encounter the difficulty of maintaining the zero-R_L bias condition over the cryostat wiring which has a finite transmission line impedance Z_0 and a finite propagation delay. One possibility is to use the room temperature amplifier which provides active Z_0 –termination of the cryostat wiring , and then to choose the $\mathcal{G}_V$ / $\mathcal{G}_I$ ratio such that $R_{D,eff}$ matches Z_0. Keeping the ratio fixed, loop gains can then be adjusted to either boost the signal power at the SQUID output at the cost of decreasing flux range, or to improve linearity at the cost of decreasing signal power.

5. Conclusion

The current-sampling negative feedback functions in practice in the way suggested by theory. A modest loop gain and the consequent modest extent of linearization is achievable in practical circuits. Larger loop gains are hindered by the associated reduction of signal power at the SQUID output which would require a readout amplifier with an extremely low noise temperature and some way to avoid the Johnson noise generated in the resistive cryostat wiring. The dynamic range in the order of $D_{0.01\mathrm{dB}} = 10^6$ $\mathrm{Hz}^{1/2}$ required by X-ray calorimeter setups [8] appear to be within the reach of the current-sampling feedback approach when combined with an additional linearization scheme, e.g. a calibrate-and-correct scheme.

Acknowledgements

Illuminating discussions about the linearity questions with Jan van der Kuur and Piet de Korte are gratefully acknowledged. This work was supported by the Centre of Excellence for Low Temperature Quantum Phenomena by the Academy of Finland.

References.

[1] Drung D, Cantor R, Peters M, Scheer H J and Koch H 1990 Low-noise high-speed dc superconducting quantum interference device

magnetometer with simplified feedback electronics *Appl. Phys. Lett*. **57** 406-8.
[2] Seppä H, Ahonen A, Knuutila J, Simola J and Vilkman V 1991 dc SQUID electronics based on adaptive positive feedback: experiments *IEEE Tran. Magn.* **27** 2488-90.
[3] Seppä H 1992 Dc SQUID electronics based on adaptive noise cancellation and a high open-loop gain controller *Superconducting devices and their applications (SQUID'91)* H. Koch and H Lübbig, editors, 346-50.
[4] Forgacs R L and Warnick A 1966 Lock-on magnetometer utilizing a superconducting sensor *IEEE Tran. Instr. Meas.* **IM-15** 113-20.
[5] Millman J 1979 *Microelectronics* McGraw-Hill Tokyo.
[6] M. Kiviranta and H. Seppä 1999 Comparison of dc SQUID readout methods based on positive feedback *Extended abstracts of 7th International Superconductive Electronics Conference (ISEC'99)* 158-60.
[7] van der Kuur J, Kiviranta M and de Korte P 2003 *SRON-CIS-Rep-WP-511 report* 44-5, unpublished.
[8] de Korte P et. al. 2006 EURECA – a european-japanese micro-calorimeter array *Proc. SPIE* **6266** 62661Z.
[9] van der Kuur J 2005, private communication.
[10] Hahn I, Day P, Limketkai B, Bumble B and Leduc H G 2008 Recent results of a new microwave SQUID multiplexer, to appear in *J. Low Temp. Phys*. DOI 10.1007/s10909-008-9773-y.
[11] Lehnert K W, Irwin K D, Castellanos-Beltran M A, Mates J A B and Vale L R 2007 Evaluation of a microwave SQUID multiplexer prototype *IEEE Tran. Appl. Supercond.* **17** 705-9.
[12] Drung D and Koch H 1993 An electronic second-order gradiometer for biomagnetic applications in clinical shielded rooms *IEEE Tran. Appl. Supercond.* **3** 2594-7.
[13] Kiviranta M and Seppä H 1995 Dc SQUID electronics based on the noise cancellation scheme *IEEE Tran. Appl. Supercond.* **5** 2146-8.
[14] Kiviranta M 2008 High dynamic range SQUID readout for frequency-domain multiplexers, to appear in *J. Low Temp. Phys.* DOI 10.1007/s10909-008-9765-y.
[15] Grönberg L, Hassel J, Helistö P, Kiviranta M, Seppä H, Kulawski M, Riekkinen T and Ylilammi M 2005 Fabrication process for millikelvin Josephson junction circuits *Extended abstracts of 10th International Superconductive Electronics Conference (ISEC2005)* O-W.04 .
[16] Kiviranta M 2006 Use of SiGe bipolar transistors for cryogenic readout of SQUIDs *Supercond. Sci. Tech.* **19** 1297-1302.